Journal of Physics: Condensed Matter

Formation of a spin density wave in copper metaborate by a spin polaron

To cite this article: S S Aplesnin 2004 *J. Phys.: Condens. Matter* **16** 5907

INSTITUTE OF PHYSICS PUBLISHING JOURNAL OF PHYSICS: CONDENSED MATTER

J. Phys.: Condens. Matter **16** (2004) 5907–5914 PII: S0953-8984(04)81559-5

Formation of a spin density wave in copper metaborate by a spin polaron

S S Aplesnin

Kirensky Institute of Physics, Siberian Branch of the Russian Academy of Sciences, Krasnoyarsk, 660036, Russia

E-mail: apl@iph.krasn.ru

Received 2 June 2004
Published 30 July 2004
Online at stacks.iop.org/JPhysCM/16/5907
doi:10.1088/0953-8984/16/32/023

Abstract

Formation of incommensurate three-dimensional magnetic order below $T^* \sim 10$ K in CuB_2O_4 is explained on the basis of strong correlation between the holes and localized spins. The Kondo lattice model is analysed for the case where spin polarons are the elementary excitations. The origin of the low-temperature specific heat maximum at $T \sim 5$ K is associated with a displacement of the polaron band bottom. A set of anomalies in the temperature dependence of the conductivity, shift of the optical conductivity maximum in the range of energies 0.02–0.12 eV and decreasing of the infrared absorption intensity is predicted.

(Some figures in this article are in colour only in the electronic version)

1. Introduction

The formation of incommensurate structures has often been observed in low-dimensional spin $S = 1/2$ systems as in $RbCuCl_3$ [1] and a field-induced magnetic soliton lattice in the spin–Peierls compounds $CuGeO_3$ [2]. The formation origin of incommensurability is a competition of different interactions: antiferromagnetic exchanges between nearest and next-nearest neighbours, Dzyaloshinskii–Moriya interactions and interaction between magnetic systems and elastic or electron systems with an incommensurate period of structure.

The incommensurate structure in a three-dimensionally ordered magnetic lattice is found in CuB_2O_4 [3]. Upon lowering the temperature below $T^* < 10$ K, a second magnetic phase transition toward an incommensurate three-dimensional magnetic order occurs. In the incommensurate phase, but in the vicinity of T^*, higher-order satellites appear in the neutron diffraction pattern. CuB_2O_4 crystallizes in space group $I\bar{4}2d$ (D_{2d}^{12}) with lattice constants $a = 11.528$ Å, and $c = 5.607$ Å [4]. The existence of such magnetic structure has been explained by relativistic effects such as spin–orbit coupling that is ascribed to a kind of

Dzyaloshinskii–Moriya (DM) interaction. Using the DM interaction and anisotropy in the basal plane the modulation of the order parameter in copper metaborate along the helix direction is described within the Landau theory of phase transitions by the solution of the sine–Gordon equation. Treatment of inelastic scattering neutron using spin wave theory gives magnetic moment per site $\sigma = 0.94\ \mu_B$ and antiferromagnetic exchange between nearest neighbours $J = 3.93 \pm 0.02$ meV [5]. The Nèel temperature is $T_N = 20$ K, the paramagnetic Curie temperature is $\Theta = -9.5$ K and an effective magnetic moment determined from the magnetic susceptibility is $\mu_{eff} = 1.77\ \mu_B$ [6].

2. Model

In this paper we suggest a microscopic theory of formation of incommensurate magnetic structure in CuB_2O_4. On the basis of the results of the theory the unclear origin of the low-temperature specific heat maximum [10] and a discrepancy between exchange values determined at low and high temperatures from the paramagnetic Curie temperature $I = 3\Theta/(zS(S+1)) \simeq 0.9$ meV will be explained. CuB_2O_4 reveals slight piezoelectric properties [7]. So single-axis pressure along [011] induces a electrical induction. The acoustic transverse waves expanded along [100] show anisotropy of velocities $v_{010} = 4867.7 \pm 0.1$, $v_{001} = 5307.0 \pm 0.5$ m s^{-1} for wave polarization [010] and [001] [7]. These results suggest the existence of anisotropy of the electron density distribution within ∼8%.

We suppose the electrical properties of copper metaborate are attributable to the bounded state of the electron and hole. The energy difference term of copper and boron ions Cu^{2+}, B^{3+} is $\Delta(E_{B^{3+}} - E_{Cu^{2+}}) \sim 1$ eV [8] and they connect by means of the oxygen. As a result of this the effective charge of copper may increase and the charge of boron may decrease. This may be interpreted as the formation of a hole in a copper ion. The strong hole interaction with the excitations of the antiferromagnetically ordered spin subsystem is described in terms of the s–d model. In this case, a more complex excitation—a spin polaron—is a good quasiparticle.

In the currently existing theoretical studies the energetically low-lying spin-polaron states are constructed first to calculate the elementary excitation bands. The mean-field approach is applied to the simplest model of the Kondo lattice [9]. The Hamiltonian of this is

$$\begin{aligned} H &= H_0 + H_1 + H_2, \\ H_0 &= \sum_{\mathbf{r},\mathbf{g}} (t_{\mathbf{h_p}} a^{\dagger}_{\mathbf{r}+\mathbf{h_p},\sigma} a_{\mathbf{r},\sigma} + t_{\mathbf{h_c}} a^{\dagger}_{\mathbf{r}+\mathbf{h_c},\sigma} a_{\mathbf{r},\sigma} + e.c.) = \sum_{\mathbf{k}} \varepsilon_{\mathbf{k}} a^{\dagger}_{\mathbf{k},\sigma} a_{\mathbf{k},\sigma}, \\ H_1 &= J \sum_{\mathbf{r},\sigma_1,\sigma_2} a^{\dagger}_{\mathbf{r},\sigma_1} S^{\alpha}_{\mathbf{r}} \hat{\sigma}^{\alpha}_{\sigma_1,\sigma_2} a_{\mathbf{r},\sigma_2}, \\ H_2 &= \tfrac{1}{2} I \sum_{\mathbf{r},\mathbf{g}} S^{\alpha}_{\mathbf{r}+\mathbf{g}} S^{\alpha}_{\mathbf{r}}. \end{aligned} \tag{1}$$

Here, the sites $\mathbf{r}$ form a tetragonal lattice, h_p and h_c are the distances to the nearest neighbours in the plane and along the c-axis, $a^{\dagger}_{\mathbf{k},\sigma}$ is the creation operator for the holes with spin indices $\sigma = \pm 1$, H_0 describes the carrier hopping, $t_{\mathbf{h_p}} = -t_1$, $t_{\mathbf{h_c}} = -t_0$, H_2 is the antiferromagnetic interaction of the localized spins $S = 1/2$ with their nearest neighbours, H_1 is the Hamiltonian of the on-site Kondo interaction, $\hat{\sigma}^{\alpha}$ are the Pauli matrices, and $\alpha = x, y, z$.

Let us write the first two equations for the Green functions describing the hole motion on the antiferromagnetic background. Using the random phase approximation the set of equations for the Green functions $\langle\langle a_{\mathbf{r},\sigma} | a^{\dagger}_{\mathbf{r},\sigma} \rangle\rangle$ and $\langle\langle b_{\mathbf{r},\sigma} | a^{\dagger}_{\mathbf{r},\sigma} \rangle\rangle$, $b_{\mathbf{r}\sigma} = S^{\alpha}_{\mathbf{r}} \hat{\sigma}^{\alpha}_{\sigma,\sigma_1} a_{\mathbf{r},\sigma_1}$, $\alpha = x, y$ is closed.

These equations have the following form:

$$
\begin{aligned}
&(\omega - \varepsilon_{\mathbf{k}})G^1_{\mathbf{k}} = 1 + \frac{J}{2}G^2_{\mathbf{k}},\\
&(\omega - e_{\mathbf{k}})G^2_{\mathbf{k}} = J(1 + m - 2nm)G^1_{\mathbf{k}},\\
&G^1_{\mathbf{k}} = \langle\langle a_{\mathbf{k},\sigma}|a^{\dagger}_{\mathbf{k},\sigma}\rangle\rangle; \qquad G^2_{\mathbf{k}} = \langle\langle b_{\mathbf{k},\sigma}|a^{\dagger}_{\mathbf{k},\sigma}\rangle\rangle\\
&\varepsilon_{\mathbf{k}} = \varepsilon^0_{\mathbf{k}} + \frac{Jm}{4} - \mu,\\
&\varepsilon^0_{\mathbf{k}} = -2t_1(\cos k_x + \cos k_y) - 2t_0 \cos k_z,\\
&e_{\mathbf{k}} = 2zc\varepsilon^0_{\mathbf{k}} + J\left(\frac{m}{2} + n\right) + \frac{z}{2}mI - \mu,\\
&n = \langle a^{\dagger}_{\uparrow}a_{\uparrow} + a^{\dagger}_{\downarrow}a_{\downarrow}\rangle.
\end{aligned}
\tag{2}
$$

Here, $b_{\mathbf{k},\sigma}$, $a_{\mathbf{k},\sigma}$ and $G_{\mathbf{k}}$ are the Fourier transforms of the corresponding on-site operators and the Green function, respectively, $c = \langle S^x_{\mathbf{r}}S^x_{\mathbf{r+g}} + S^y_{\mathbf{r}}S^y_{\mathbf{r+g}}\rangle$ is the spin–spin correlation function on the transverse spin components, z is the number of nearest neighbours, and m is the sublattice magnetization. All energies are reckoned from the chemical potential μ.

The solution to the set of equations (2) leads to the following excitation spectrum:

$$
\omega_{1,2}(\mathbf{k}) = \frac{1}{2}\left[\varepsilon_{\mathbf{k}} + e_{\mathbf{k}} \pm \sqrt{(\varepsilon_{\mathbf{k}} - e_{\mathbf{k}})^2 + J^2\left(\frac{1+m}{2} - nm\right)}\right]. \tag{3}
$$

The chemical potential is calculated from the self-consistent solution of the equation for the hole concentration n

$$
n = \frac{1}{N}\sum_{\mathbf{k}}\int \mathrm{d}\omega\, f(\omega)\frac{1}{\pi}\,\mathrm{Im}\,G^1, \tag{4}
$$

where $f(\omega) = (\exp(\omega/T) + 1)^{-1}$. The summation over the momentum in the Brillouin zone is made using 8×10^6 points.

To calculate the self-consistent sublattice magnetization and spin–spin correlation function we write four additional linear differential equations for the Green functions $\langle\langle S^{\alpha}_{\mathbf{r},\gamma}|b_{\mathbf{r},\sigma}\rangle\rangle$, $\langle\langle S^{\alpha}_{\mathbf{r},\gamma}|S^{\alpha}_{\mathbf{r},\gamma'}\rangle\rangle$ for the two sublattices $\gamma, \gamma' = 1, 2$, and two equations for the sublattice magnetization and correlation function. The task can be simplified if we consider the magnetic system in the adiabatic approximation and make some estimations for the temperature dependence of m, c. The free energy expansion procedure gives the power function $m = m_0\sqrt{1 - T/T_{\mathrm{N}}}$. According to the elastic neutron scattering data [3] the sublattice magnetization is $m_0 = 0.94\ \mu_{\mathrm{B}}$ at $T = 2$ K. The spin–spin correlation function for the nearest neighbour sites may be estimated at the Néel temperature as

$$
\langle S^{\alpha}_0 S^{\alpha}_r\rangle \simeq \frac{\langle (S^{\alpha})^2\rangle}{1+r} = \frac{S(1+S)}{3(1+r)}; \qquad \langle S^{\alpha}_0 S^{\alpha}_{r=1}\rangle = 0.125. \tag{5}
$$

At low temperatures when the correlation radius of the spin fluctuations is $\xi \sim a$ (a—lattice constant) the transverse spin–spin correlation function is calculated in the mean-field approximation $\langle S^{\alpha}_0 S^{\alpha}_{r=1}\rangle = 0.125(1-m^2)$. The dependence of $c(T)$ in the paramagnetic phase is taken to be symmetric relative to the Nèel temperature.

As a result of the anisotropy of the transverse acoustic waves, the piezoelectric constants in CuB_2O_4 and the tetragonal symmetry a (lattice constant in plane) $> c$ the carrier hoppings should also be taken as anisotropic, $t_1/t_0 = 0.92$.

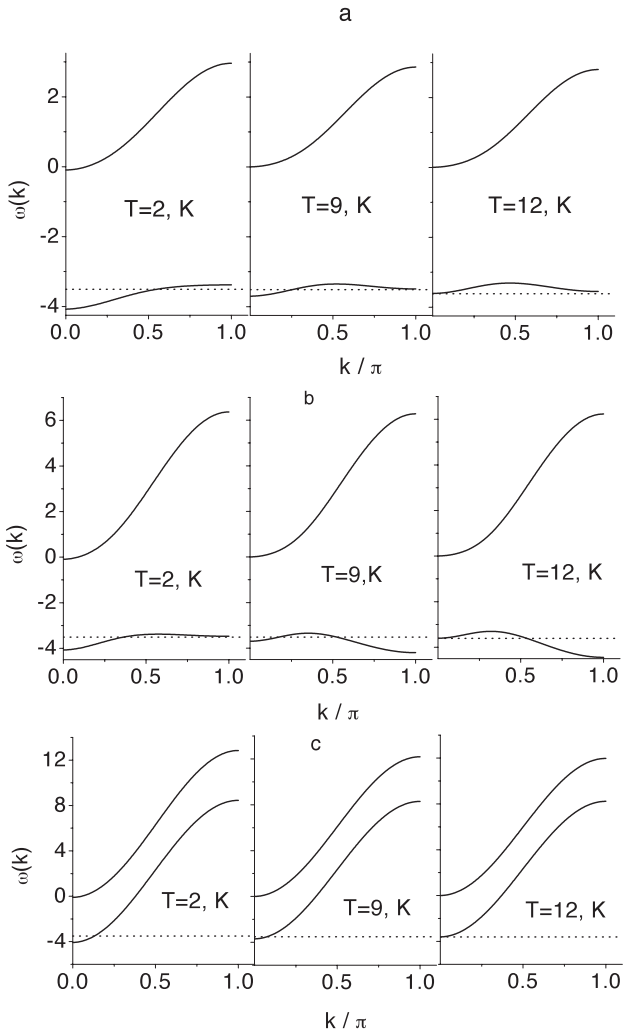

Figure 1. Dispersion branches of spin-polaron excitations along [001] (a); [101] (b); [111] (c) at different temperatures. The horizontal line indicates the position of the chemical potential in the lower band (dotted line).

3. Discussion of results

The polaron excitation spectra for three directions are shown in figure 1 for the following parameters: $I/t_0 = 0.08$, $J/t_0 = 2.06$. The band splitting of free electrons is observed in consequence of the strong interaction with the localized spins forming an ordered Nèel state. The Fermi level locates in the lower band near the chemical potential denoted in figure 1 by a dotted line. The Fermi energy and s–d energy of interaction have comparable values. S-electrons form a spin density wave (SDW) with the wavevector arranged near the Fermi surface since the Fermi energy exceeds by more than one order of magnitude the magnetic excitation energy. SDW modulates the density of localized spins that causes the additional satellites observed in the neutron diffraction pattern. The evolution of the satellite position

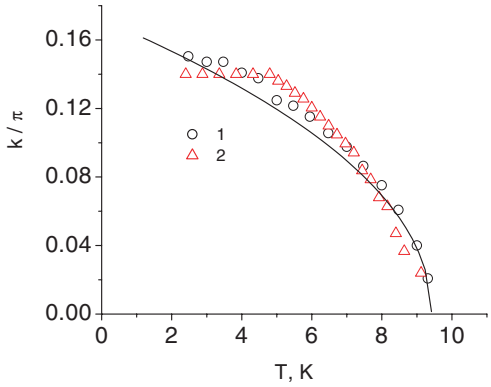

Figure 2. The temperature dependence of Fermi momentum (2) and the satellite position in the neutron diffraction pattern (1). The curve is the fitting function $Q(T) \sim (T^* - T)^{0.48}$ [3].

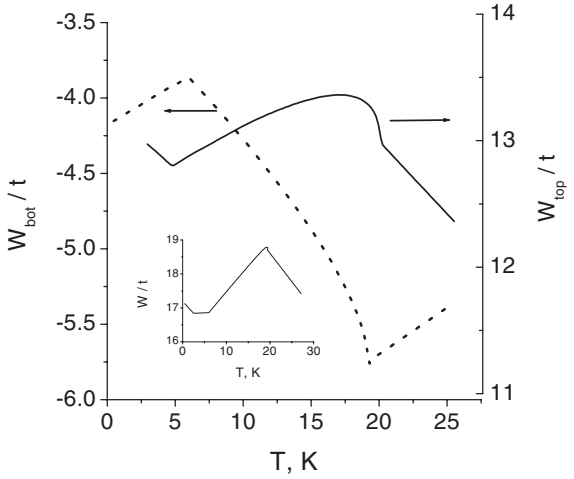

Figure 3. The energy of the band bottom W_{bot}/t and band top W_{top}/t versus the temperature. The inset illustrates the temperature dependence of the bandwidth.

with temperature is found to follow a power law [3]

$$Q(T) \propto (T^* - T)^{\nu}, \tag{6}$$

with $\nu = 0.48$, as shown in figure 2. The calculated change of Fermi momentum k_{F} along [001] (figure 2) versus temperature is in good agreement with the experimental data. The estimated value of $k_{\mathrm{F}} = (0, 0, 0.14)$ at $T = 1.8$ K is also in accord with the period of the spin modulation, $Q = (0, 0, 0.15)$. The Fermi surface is a restricted domain with the centre of the band at $T < T^*$ and vanishes at $T = T^*$. The Fermi momentum lies in the range of $\pi/2 < k_{\mathrm{F}} < \pi$ with centres on the band edges where the spin-wave spectrum in CuB_2O_4 is not observed. The decrease of the effective interaction energy of s electrons with the localized spins caused by decreasing sub-lattice magnetization results in a shift of the bottom and top of the polaron band and an increase of the bandwidth as shown in figure 3. In the paramagnetic phase the rise of the antiferromagnetic correlations on cooling also leads to an increase of the bandwidth.

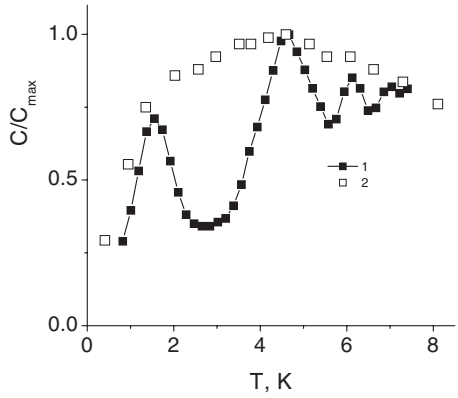

Figure 4. Temperature dependence of the specific heat normalized to the maximum value induced by spin polarons (1) and experimental data (2) [10].

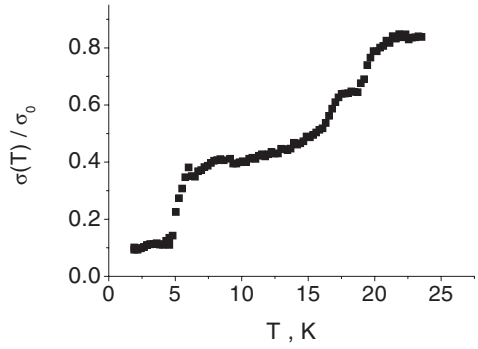

Figure 5. Temperature dependence of the conductivity $\sigma(T)$ at $\omega \to 0$.

To estimate the contribution of the polaron excitations to the specific heat the average value of the kinetic energy of the polaron K_p is simulated by the Green function

$$K_\mathrm{p} = \frac{1}{N}\sum_{\mathbf{k}} \omega(\mathbf{k}) \frac{1}{\pi} \int \mathrm{d}E\, f(E)\, \mathrm{Im}\, G_2(\mathbf{k}, E). \tag{7}$$

The temperature dependence of $C = \mathrm{d}K_\mathrm{p}/\mathrm{d}T$ is plotted in figure 4. Specific heat maxima are observed at $T \simeq 1.7$, 4.5 K. Temperatures corresponding to the specific heat maxima agree well with experimental data [10] as shown in figure 4. Transport properties such as conductivity can be obtained from Kubo formulae in the limit of $d \to \infty$ [11]

$$\begin{aligned} \sigma(\omega) &= \sigma_0 \sum_{\sigma} \int \mathrm{d}\omega'\, I_\sigma(\omega', \omega' + \omega) \frac{f(\omega') - f(\omega' + \omega)}{\omega}, \\ I_\sigma(\omega_1, \omega_2) &= \frac{1}{\pi^2} \sum_{\mathbf{k}} \mathrm{Im}\, G_\sigma(\mathbf{k}, \omega_1)\, \mathrm{Im}\, G_\sigma(\mathbf{k}, \omega_2) \end{aligned} \tag{8}$$

where σ_0 is a constant defining a dimension of conductivity. The temperature dependence of the conductivity $\sigma(\omega \to 0)$ is presented in figure 5. Below T_N the magnitude of σ decreases sharply with increasing sublattice magnetization. At $T \sim 16$ K the change of the derivative sign of the chemical potential from $\mathrm{d}\mu/\mathrm{d}T < 0$ to $\mathrm{d}\mu/\mathrm{d}T > 0$ correlates with the peculiarity in $\mathrm{d}\sigma/\mathrm{d}T$. The drop of the conductivity at $T > 5$ K arises from the shift of band bottom

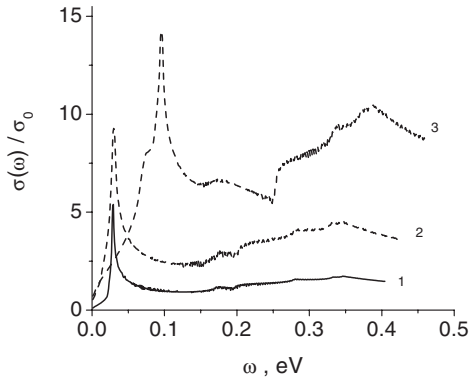

Figure 6. Optical conductivity at temperatures $T = 2$ K (1), 7 K (2), and 17 K (3).

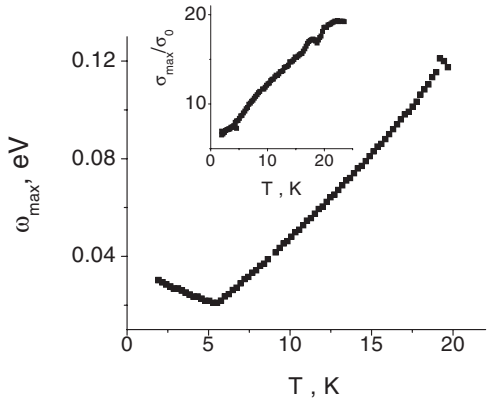

Figure 7. Energy $\omega_{\max}$ associated with the maximum value of the optical conductivity $\sigma_{\max}$ versus temperature. The inset illustrates $\sigma_{\max}$ versus temperature.

minimum from the zone centre $(0, 0, 0)$ to $(1, 0, 1)$, $(0, 1, 1)$. This is shown in figure 1(b). The optical conductivity is presented in figure 6 and reveals two maxima. The first peak results from intraband transitions and the broad maximum $\sigma(\omega)$ is attributed to transitions between the lower and upper bands. The energy corresponding to the first peak and the intensity versus the temperature are shown in figure 7. The temperature dependence of $\sigma(T)$ may be observed by microwaves for an amplitude of electric field E_0 and a plane polarized wave with frequency ω. The absorption power delivered to the system is defined as $P(\omega) = \frac{1}{2}E_0^2 \operatorname{Re}[\sigma_z(\omega)]$ [12]. A decrease of intensity of the infrared absorption in CuB_2O_4 can be found at $T < T_N$ and at $\omega \sim 0.4$ eV.

The features in the low-temperature behaviour of the specific heat and conductivity arise from a modification of the polaron excitation band. The density of state maximum is near the Fermi level and shifts to high energies at $T > 10$ K. Increasing hole concentration leads to a decrease of the critical temperature for formation of spin structure modulation T^*. The specific heat maximum also shifts to low temperatures. These concentration dependences are given in figure 8. Displacement of the B^{3+} ion in CuB_2O_4 by a bivalent ion induces a rise of hole concentration and leads to a decrease of critical temperature T^*. A similar effect may be observed in a nonuniform electric field because a electron–hole coupling pair

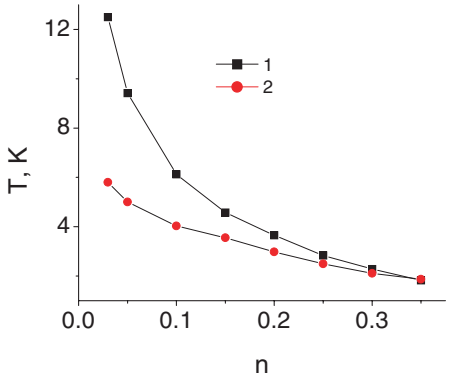

Figure 8. Critical temperature of formation of the spin density wave $T^*(1)$ along [001] and the temperature corresponding to the specific heat maximum $T_{C_{\max}}(2)$ versus hole concentration.

will move and the difference between the kinetic and effective potential energy due to s–d exchange decreases. Holes hopping between nearest neighbours gives rise to the appearance of additional ferromagnetic exchange and as a result of the total exchange at $T \gg T_N$ decreases in comparison with the exchange value at $T \ll T_N$.

4. Conclusion

In conclusion, we summarize the main results. Spin polarized s-electrons form a spin density wave with the period equal to the Fermi momentum. The SDW modulates the density of localized spins as a result of strong s–d coupling. The estimated temperature dependence of the spin polaron Fermi momentum is in good agreement with the evolution of the satellite position versus temperature in CuB_2O_4. The low-temperature specific heat maximum arises from the shift of the band bottom minimum from the zone centre (0, 0, 0) to (1, 0, 1), (0, 1, 1). The presented calculations predict a sharp decrease of the conductivity and the intensity of infrared absorption at the Nèel temperature and a drop of conductivity at $T \simeq 5$ K.

References

[1] Maruyama S, Tanaka H and Narumi Y 2001 *Preprint* cond-mat/0010388
[2] Horvatic M *et al* 1999 *Phys. Rev. Lett.* **83** 420
[3] Roessli B *et al* 2001 *Phys. Rev. Lett.* **86** 1885
[4] Martinez-Ripoli M *et al* 1971 *Acta Crystallogr.* B **27** 677
[5] Boehm M *et al* 2002 *J. Magn. Magn. Mater.* C **250** 313
[6] Petrakovskii G A, Balaev A D and Vorotinov A M 2000 *Phys. Solid State* **42** 321
[7] Aleksandrov K S *et al* 2003 *Phys. Solid State* **45** 467
[8] Bergmann D and Hinze J 1996 *Angew. Chem. Int. Edn Engl.* **35** 150
[9] Barabanov A F, Maksimov L A and Mikheenkov A V 2001 *JETP Lett.* **74** 362
[10] Petrakovskii G A, Popov M A and Roessli B 2001 *JETP* **92** 809
[11] Izyumov Ya A and Skryabin Yu N 2001 *Phys.—Usp.* **44** 121
[12] Ando T, Fowler A B and Stern F 1982 *Rev. Mod. Phys.* **54** 437